UC Santa Barbara
UC Santa Barbara Previously Published Works

Title

Time-dependent evolution of functional vs. remodeling signaling in induced pluripotent stem cell-derived cardiomyocytes and induced maturation with biomechanical stimulation

Authors

Jung, Gwanghyun
Fajardo, Giovanni
Ribeiro, Alexandre JS
et al.

Peer reviewed

Time-dependent evolution of functional *vs.* remodeling signaling in induced pluripotent stem cell-derived cardiomyocytes and induced maturation with biomechanical stimulation

Gwanghyun Jung,*,† Giovanni Fajardo,*,† Alexandre J. S. Ribeiro,‡ Kristina Bezold Kooiker,*,† Michael Coronado,*,† Mingming Zhao,*,† Dong-Qing Hu,*,† Sushma Reddy,*,† Kazuki Kodo,†,§ Krishna Sriram,¶ Paul A. Insel,¶ Joseph C. Wu,†,§,‖ Beth L. Pruitt,‡ and Daniel Bernstein*,†,1

*Division of Cardiology, Department of Pediatrics, †Stanford Cardiovascular Institute, §Division of Cardiovascular Medicine, Department of Medicine, and ‖Institute for Stem Cell Biology and Regenerative Medicine, Stanford University School of Medicine, Stanford, California, USA; ‡Department of Mechanical Engineering, Stanford University School of Engineering, Stanford, California, USA; and ¶Departments of Pharmacology and Medicine, University of California, San Diego, San Diego, California, USA

ABSTRACT   Human induced pluripotent stem cell-derived cardiomyocytes (hiPSC-CMs) are a powerful platform for uncovering disease mechanisms and assessing drugs for efficacy/toxicity. However, the accuracy with which hiPSC-CMs recapitulate the contractile and remodeling signaling of adult cardiomyocytes is not fully known. We used β-adrenergic receptor (β-AR) signaling as a prototype to determine the evolution of signaling component expression and function during hiPSC-CM maturation. In "early" hiPSC-CMs (less than or equal to d 30), β2-ARs are a primary source of cAMP/PKA signaling. With longer culture, β1-AR signaling increases: from 0% of cAMP generation at d 30 to $56.8 \pm 6.6\%$ by d 60. PKA signaling shows a similar increase: $15.7 \pm 5.2\%$ (d 30), $49.8 \pm 0.5\%$ (d 60), and $71.0 \pm 6.1\%$ (d 90). cAMP generation increases 9-fold from d 30 to 60, with enhanced coupling to remodeling pathways (*e.g.*, Akt and Ca^{2+}/calmodulin-dependent protein kinase type II) and development of caveolin-mediated signaling compartmentalization. By contrast, cardiotoxicity induced by chronic β-AR stimulation, a major component of heart failure, develops much later: 5% cell death at d 30 *vs.* 55% at d 90. Moreover, β-AR maturation can be accelerated by biomechanical stimulation. The differential maturation of β-AR functional *vs.* remodeling signaling in hiPSC-CMs has important implications for their use in disease modeling and drug testing. We propose that assessment of signaling be added to the indices of phenotypic maturation of hiPSC-CMs.—Jung, G., Fajardo, G., Ribeiro, A. J. S., Kooiker, K. B., Coronado, M., Zhao, M., Hu, D.-Q., Reddy, S., Kodo, K., Sriram, K., Insel, P. A., Wu, J. C., Pruitt, B. L., Bernstein, D. Time-dependent evolution of functional *vs.* remodeling signaling in induced pluripotent stem cell-derived cardiomyocytes and induced maturation with biomechanical stimulation. *FASEB J.* 30, 1464–1479 (2016). www.fasebj.org

Since the breakthrough techniques to generate induced pluripotent stem cells (iPSCs) (1), rapid advances have occurred in their use to elucidate previously unknown disease mechanisms and to provide a platform for assessing drug efficacy and toxicity. Studies using human induced pluripotent stem cell-derived cardiomyocytes (hiPSC-CMs) developed from patients with genetic cardiovascular disorders (*e.g.*, long QT, Timothy and Barth syndromes, and hypertrophic and dilated cardiomyopathies) have demonstrated that this platform can recapitulate many of the phenotypic abnormalities of these diseases (2–6). Prior studies have largely relied on evidence of cell contraction, sarcomeric protein expression and alignment [troponin T, α-actinin, and myosin heavy chain (MHC)], and on functional analyses (*e.g.*, inotropy, chronotropy, and induction of dysrhythmias) to define the cardiac phenotype (7). There is also growing enthusiasm for using patient-derived hiPSC-CMs as a platform to screen new drugs (*e.g.*, for treating heart failure or arrhythmia or

identifying cardiotoxicity of antineoplastic agents). However, knowledge has lagged regarding the expression and function of signaling pathways that mediate alterations in cardiac function and remodeling of CMs. Many phenotypic features of hiPSC-CMs suggest that these cells are immature, resembling embryonic or fetal more than adult CMs (8). For hiPSC-CMs to be useful in disease modeling or drug screening, it is critical to understand how closely their key cell signaling systems recapitulate those of mature human CMs. Studies conducted before key signaling pathways are expressed and functional could produce incomplete or erroneous conclusions about disease mechanisms or drug efficacy/toxicity.

Signaling through the β-adrenergic receptor (β-AR) system has been utilized as a prototype to model the function of the >800 GPCRs expressed in human tissues (9). In CMs, β-AR signaling is a primary mechanism for regulating cardiac function, coupling catecholamine stimulation to G-protein/adenylyl cyclase (ADCY) activation of PKA and its downstream targets [*e.g.*, phospholamban (PLN) and troponin I (TnI)], and enhancing contractility through alterations in $[Ca^{2+}]_i$ or in the Ca^{2+} sensitivity of contractile proteins (10).

β-AR signaling also plays a critical role in cardiac remodeling. Sustained β-adrenergic stimulation has deleterious effects on CM structure, inducing pathologic hypertrophy and cell death (11). Differences in β-AR subtype coupling to Gs/Gi proteins, down-regulation–associated signaling through β-arrestin, and interaction with pathways such as Ca^{2+}/calmodulin-dependent protein kinase type II (CaMKII), MAPKs, and PI3K-Akt mediate the balance between cardiotoxicity and cardioprotection (12). β-AR blockers, which target these pathways, have been one of the most effective classes of drugs to treat heart failure, where excessive β-AR signaling is a cardinal finding (13).

Despite the critical role of β-AR signaling in regulating CM function and structure, there are limited data regarding this signaling pathway in hiPSC-CMs. Based on prior work suggesting immaturity of β-AR signaling immediately after differentiation and a time-dependent transition of subtype-specific activity after cardiac induction (14, 15), we aimed to define the development of β-AR signaling in hiPSC-CMs and the role of β-AR signaling in cardiotoxicity and remodeling, which has not previously been studied in hiPSC-CMs. Additionally, most prior knowledge of β-AR signaling comes from studies on rodent CMs for which findings can be difficult to extrapolate to humans. Prior studies on human tissue have used transplant donor hearts (typically after severe systemic injury) or from patients with end-stage cardiomyopathy, both settings in which excessive sympathetic stimulation may dramatically alter β-AR signaling. Thus, hiPSC-CMs also represent an opportunity to correlate the cell signaling in rodent CMs with that in nondiseased human CMs.

To gain insight into the development and maturation of GPCR cell signaling in hiPSC-CMs, we thus utilized the β-AR pathway as a prototype and to examine the establishment of the complex dual role of β-AR signaling in regulating cardiac function and remodeling during hiPSC-CM maturation after cardiac induction: *1*) which components of the β-AR signaling system are expressed (Are all the parts present?); *2*) whether β-ARs couple to downstream functional and remodeling effectors that regulate function and remodeling (Do the parts work normally?); and *3*) whether β-ARs down-regulate in response to chronic stimulation (Are the normal physiologic regulatory mechanisms present?). Finally, to address concerns about the need for prolonged periods of hiPSC-CM culture, we sought to determine whether maturation of cell signaling in hiPSC-CMs can be accelerated using culture conditions that induce biomechanical patterning.

MATERIALS AND METHODS

Generation and differentiation of hiPSC-CMs

All protocols were approved by the Stanford University institutional review board. In brief, control human-induced pluripotent stem cells (hiPSCs; screened for known cardiomyopathy mutations) were generated from dermal fibroblasts and reprogrammed using the 4 Yamanaka factors (Oct4, Sox2, Klf4, and c-*myc*) delivered by Sendai virus, as described previously (16). hiPSCs were cultured on Matrigel-coated tissue culture dishes (BD Biosciences, San Jose, CA, USA) with E8 medium (Life Technologies, Gaithersburg, MD, USA). Established hiPSCs exhibited positive immunostaining for the embryonic stem cell markers SSEA-4, TRA-1-81, OCT4, and NANOG, and subsequently, teratoma formation assays yielded cellular derivatives of all 3 germ layers *in vitro* and *in vivo*, confirming the pluripotent nature of the hiPSCs (5). hiPSC lines were differentiated into hiPSC-CMs using a monolayer differentiation protocol (17). Briefly, hiPSCs were replated on Matrigel-coated plates in E8 media containing 5 µM Y27632 (ROCK inhibitor; Selleckchem, Houston, TX, USA) for further differentiation. Next, cells with 90% confluence were treated for 2 d (d 1–2) with 8 µM CHIR99021 (GSK3 inhibitor; Selleckchem) followed by 5 µM Inhibitor of Wnt response-1 (Sigma-Aldrich, St. Louis, MO, USA) treatment (d 3–4) in RPMI 1640 plus B27 (without insulin) (Life Technologies). On d 2 and 5–6, cells were placed on RPMI plus B27 (without insulin). From d 7, cells were placed on RPMI plus B27 (plus insulin) until beating was observed (around d 10). At this point, cells were glucose starved for 5 d to purify hiPSC-CMs and changed every other day in RPMI plus B27 (plus insulin) and 4% fetal bovine serum. When replating hiPSC-CMs for experiments, cells were dissociated with TrypLE (Life Technologies) and seeded on Matrigel-coated plates. Days of hiPSC-CMs in culture were counted as d 30 and 60 with a ±5 d range and as d 90 with +0–20 d range after initial cardiac induction.

Quantitative RT-PCR

Total RNA was isolated from hiPSC-CMs and human heart tissues according to the manufacturer's protocol (RNeasy Mini Kit;

Qiagen, Valencia, CA, USA). Fetal heart tissue (10.5 and 12 wk) was acquired from medical waste (StemExpress, Placerville, CA, USA). Left ventricular and atrial tissues were obtained from nonimplanted donor hearts. Primers were designed using PrimerBank (http://pga.mgh.harvard.edu/primerbank/) shown in **Table 1**. A total of 50 ng total RNA was reverse transcribed to cDNA and amplified over 40 cycles using the CFX384 Bio-Rad thermocycler (Hercules, CA, USA). Expression of β-ARs and other cardiac genes was confirmed in each stage of hiPSC-CMs as well as in human heart tissues for comparison. One-step quantitative RT-PCR using SYBR Green technology (Qiagen) was performed. Gene expression was normalized to the housekeeping genes glyceraldehyde-3-phosphate dehydrogenase (GAPDH) or actin and compared during differentiation of hiPSC-CMs and human heart tissues using the 2 power ($-\Delta\Delta C_\mathrm{T}$) method (18). To obtain the relative quantification between β-ARs, we followed the method provided by Qiagen. In brief, standard curves and the slope for each primer set were constructed and used for their relative expression ($\Delta\Delta C_\mathrm{T}$/slope).

GPCR microarrays

Total RNA isolated from hiPSC-CMs was converted to cDNA using SuperScript III reagent (Invitrogen, Carlsbad, CA, USA), with random hexamers used as the RT-PCR primers. GPCR mRNA expression was determined with TaqMan Human GPCR Arrays according to the manufacturer's protocol, run on an ABI Prism 7900HT system, and analyzed with the Sequence Detection System software (all from Applied Biosystems, Foster City, CA, USA). Quantification of GPCR mRNA expression was normalized relative to GAPDH mRNA.

Immunoblotting

Cells or tissue samples were homogenized, and proteins were quantified with Bradford and separated by Tris-glycine SDS/PAGE (both from Bio-Rad). Transferred proteins on nitrocellulose membrane were probed against PLN, phospho-CaMKII, sarcoplasmic reticulum Ca^{2+} ATPase (SER-CA2a) (Pierce, Rockford, IL, USA), phospho-PLN (Ser16) (EMD Millipore, Billerica, MA, USA), Na^+/Ca^{2+} exchanger 1 (NCX1), GAPDH (Abcam, Cambridge, MA, USA), calsequestrin2 (CASQ2) (Affinity BioReagents, Golden, CO, USA), TnI, phospho-TnI (Ser23/24), ERK1/2, phospho-ERK1/2, Akt, phospho-Akt, calreticulin (Cell Signaling Technology, Beverly, MA, USA), Cav1.2 (Alomone, Jerusalem, Israel), caveolin-3 (Cav3) (BD Biosciences), myosin regulatory light chain-2a, myosin regulatory light chain-2v (Synaptic Systems,

Goettingen, Germany), and β1- and β2-AR (Santa Cruz Biotechnology, Santa Cruz, CA, USA). CaMKIIδ antibodies were kindly provided by Dr. Donald M. Bers (University of California, Davis, Davis, CA, USA).

cAMP production

Intracellular cAMP concentration was measured using an enzyme-linked immunoassay (Amersham/GE Healthcare, Pittsburgh, PA, USA) after 10 min stimulation of cells with forskolin or isoproterenol (ISO) with or without β-AR subtype-selective antagonists, ICI118,551 (ICI) or CGP20712A (CGP), or with the nonselective β-AR antagonist propranolol (PRO; all from Sigma-Aldrich). Antagonists were applied for 30 min before ISO stimulation. Reactions were terminated by the addition of sulfuric acid and read at 450 nm within 30 min using the Synergy H1 hybrid microplate reader (BioTek Instruments, Winooski, VT, USA). Intracellular cAMP concentration was calculated using a standard curve (25–6400 fmol) and normalized to the amount of protein used.

Immunofluorescent confocal microscopy

hiPSC-CMs were replated on a coverslip coated with Matrigel for immunostaining. Cells were washed 3 times with ice-cold PBS, fixed with 4% paraformaldehyde in PBS for 10 min at room temperature, and permeabilized with 0.2% Triton X-100 in PBS for 5 min at room temperature. After 2 washes with PBS and blocking in solution containing 20 mM Tris-HCl (pH 7.5), 150 mM NaCl, 0.1% Tween 20, and 1% bovine serum albumin, cells were incubated with primary antibody followed by fluorescent-conjugated secondary antibody (Molecular Probes, Carlsbad, CA, USA). Imaging was performed using a Zeiss LSM 510 Meta confocal microscope using Zen imaging software (both from Carl Zeiss AG, Feldbach, Switzerland).

Receptor internalization

Flag-tagged human β1-AR (plasmid #14698) or β2-AR (plasmid #14697) in pcDNA3 vector (Addgene, Cambridge, MA, USA) was transfected into hiPSC-CMs grown on coverslips and using Lipofectamine LTX following the manufacturer's protocol (Life Technologies). One day after transfection, cells were serum starved for 4 h and then incubated with 10 μM ISO for 1 h. After 1 h incubation at 37°C, cells were fixed and permeabilized before staining with anti-Flag antibody. For the 0 min point, coverslips were fixed without stimulation.

TABLE 1. *Primers used in this study.*

Gene name	5′ Sequence	3′ Sequence
β-AR1	ATCGAGACCCTGTGTGTCATT	GTAGAAGGAGACTACGGACGAG
β-AR2	TGGTGTGGATTGTGTCAGGC	GGCTTGGTTCGTGAAGAAGTC
β-AR3	GACCAACGTGTTCGTGACTTC	GCACAGGGTTTCGATGCTG
ADCY5	TCTCCTGCACCAACATCGTG	CATGGCAACATGACGGGGA
ADCY6	GCTCATGGTGGTGTGTAACC	GCGTGTAGGCGATGTAGACAAA
CASQ2	GGCAGAAGAGGGGCTTAATTT	GAAGACACCGGCTCATGGTAG
Cav3	GACCCCAAGAACATTAACGAGG	GGACAACAGACGGTAGCACC
CaMKIIδ	GTCACTGAACAACTGATCGAAGC	GAATCGGTGAAAATCCATCCTT
MURC	GATCTGCCAGGCTTAGGAAGT	CCGGGGTCACTATTCTAGTTCTA
GAPDH	GGAGCGAGATCCCTCCAAAAT	GCTGTTGTCATACTTCTCATGG
Actin	CATGTACGTTGCTATCCAGGC	CTCCTTAATGTCACGCACGAT

MURC, muscle-restricted coiled-coil protein.

Cytotoxicity assay

hiPSC-CMs were incubated in serum-free medium for 24 h before incubation with reagents. hiPSC-CMs at different times after cardiac induction were challenged with ISO or doxorubicin (DOX) at the indicated doses. After 48 h treatment, cell viability was measured by using the CellTiter 96 AQueous Assay (Promega, Madison, WI, USA) following the manufacturer's instructions, with the conversion of tetrazolium 3-(4,5-dimethylthiazol-2-yl)-5-(3-carboxymethoxyphenyl)-2-(4-sulfophenyl)-2H-tetrazolium) into formazan at 490 nm absorbance and absorbance reading correlating directly with cell viability.

Beating rate and Ca^{2+} transient measurements

A set of hiPSC-CMs was loaded with 0.5 μM Fura 2-acetoxymethyl ester (Molecular Probes) for 15 min and washed for 30 min. Cells were excited at 340 and 380 nm, continuously alternated, at rates as high as 250 pairs per second using a HyperSwitch system (Ion-Optix Corporation, Milton, MA, USA). Background-corrected Fura 2 ratios were collected at 510 nm. This ratio is independent of cell geometry and excitation light intensity and reflects the intracellular Ca^{2+} concentration.

Fabrication of microgrooved aligned substrates and replating hiPSC-CMs on these substrates

Polydimethylsiloxane (PDMS) microgrooves were fabricated using previously reported soft lithography techniques (19, 20) with some modifications. A 10-μm–thick layer of a negative photoresist (SU-8 3010; MicroChem, Newton, MA, USA) was spin coated onto silicon wafers (mechanical grade; University Wafer, South Boston, MA, USA) for 30 s at 3500 rpm and UV exposed for 8.5 s at 20 mW/cm^2 (365 nm light source; OAI, San Jose, CA, USA) through a transparency mask (FineLine Imaging, Colorado Springs, CO, USA) and long-pass UV filter (PL-360-LP; Omega Optical, Brattleboro, VT, USA). The AutoCAD-generated transparency mask contained lines of 30 μm width and spacing between lines. Before UV exposure, SU-8 was baked on a hot plate. Before development, SU-8 was submitted to postexposure baking. After development of cured SU-8 features for 4.5 min in liquid with mild agitation (SU-8 Developer; MicroChem), N$_2$ gas-dried wafers were silanized in an atmosphere of trimethylchlorosilane (Sigma-Aldrich) for 3 h. PDMS (Dow Corning, Midland, MI, USA) prepolymer and curing agent (Thinky, Laguna Hills, CA, USA), were mixed 10:1, cast on the SU-8 aligned microgrooves, cured for 24 h at 70°C, and then peeled from the SU-8 master. Substrate surfaces were then oxidized through O$_2$ plasma treatment with 66.6 Pa and 80 W in an oxygen plasma asher (Branson/IPC-S3003; Novellus Systems Inc., San Jose, CA, USA) for 15 s and incubated overnight in a solution of Matrigel (BD Biosciences). The microgrooved PDMS substrates had microchannel dimensions of 30 μm width, 30 μm spacing, and 10 μm depth. Flat PDMS control substrates were also fabricated following the same protocol. Substrates were washed twice with L-15 medium and dried under a low stream of N$_2$ gas before seeding cells. hiPSC-CMs were cultured in RPMI plus B27/4% fetal bovine serum for 30 or 40 d. Then, hiPSC-CMs (5 $\times$ 10^4/cm^2) were replated on PDMS (microgrooved and flat) substrates and maintained with every other day changing of the medium before analysis.

Statistical analysis

Data are presented as means $\pm$ SEM. Statistical analyses were performed with GraphPad Prism (GraphPad Software Incorporated, La Jolla, CA, USA). Comparisons between 2 groups were conducted via a 2-tailed unpaired Student's t test. A 1-way or 2-way ANOVA was used to compare multiple data sets with an indicated test for pairwise comparisons; $P < 0.05$ was considered statistically significant.

RESULTS

Differential expression of β1 $vs.$ β2-ARs with time after cardiac induction of hiPSC-CMs

hiPSCs were derived from dermal fibroblasts obtained from a healthy control patient and differentiated into CMs as described in Materials and Methods (17). Prolonged culture of hiPSC-CMs results in maturation of several phenotypic characteristics (7, 21). To provide detailed information regarding the maturation of β-AR signaling, we first compared gene expression of the 3 β-AR subtypes (β1-AR, β2-AR, and β3-AR) in early (d 30 $\pm$ 5), mid (d 60 $\pm$ 5), and late (d 90 + 20) stages of hiPSC-CMs after cardiac induction (d 0). In nondifferentiated hiPSCs, overall expression of β-ARs is very low, most of which are β2-ARs; however, after cardiac induction, expression of both β1- and β2-ARs significantly increases. During the early stage (d 30), β2-ARs are the dominant subtype (94% of total β-ARs), but by d 60, a major increase in β1-AR begins. By d 90, β1-AR expression is 15-fold higher than at d 30 ($vs.$ 3-fold for β2-ARs) (**Fig. 1A, B**), resulting in a time-dependent increase in the proportion of β1-ARs (3% at d 30 $vs.$ 36% at d 90) (Fig. 1D). Comparison of the expression and ratio of β-ARs in hiPSC-CMs to those in fetal and adult human heart revealed that the ratio of β1-ARs in d 60 hiPSC-CMs was higher than in fetal heart (28 $vs.$ 15%) but at d 90 was intermediate between fetal and adult hearts, suggesting a partial recapitulation of the normal developmental pattern in the human heart. Similar to human hearts, β3-AR expression was substantially lower in hiPSC-CMs at all the time points (Fig. 1C). Protein analysis confirmed the significant increase in β1-ARs between d 30 and 60 (Supplemental Fig. S2A). To determine the generalizability of our findings to other hiPSC-CM lines, we analyzed 2 additional control hiPSC-CM lines, obtained from different individuals, and found a similar time-dependent pattern of β-AR subtype expression after differentiation (Supplemental Fig. S1).

We also quantified the protein expression of key downstream targets of β-AR signaling, as well as components responsible for Ca^{2+} signaling regulation at early, mid, and late stages (**Fig. 2B** and Supplemental Fig. S2). Maximal expression of most of the β-AR downstream partners (PLN, TnI, and Cav$_{1.2}$) and key Ca^{2+} handling proteins (SERCA2a, NCX1, and calreticulin) was established by d 30; in contrast, the sarcoplasmic reticulum (SR)-associated protein CASQ2 matured later, increasing by d 60.

Coupling of β-ARs to downstream targets mediating changes in contractile function

Upon agonist stimulation, β-ARs activate the Gs/ADCY cascade, generating the second messenger cAMP. To examine if β-ARs are functionally coupled to this pathway, we

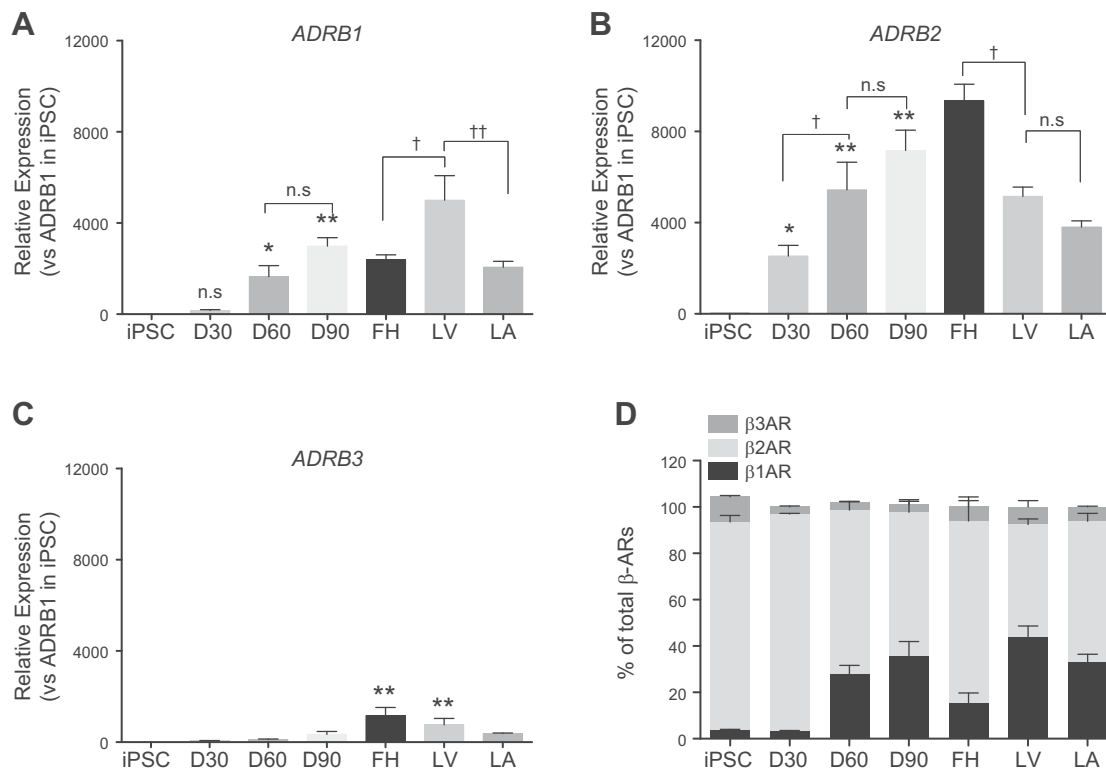**Figure 1.** Differential expression of β-AR subtypes with time after cardiac induction of hiPSC-CMs. *A–C*) Gene expression of β1- and β2-ARs increases with time following differentiation. Minimal β1-AR expression is present at d 30, but this increases dramatically by d 60. *D*) Relative ratios of β-AR subtypes in hiPSC-CMs. With increased time after differentiation, the proportion of β1-ARs increases from 3% at d 30 to 35% at d 90, partially recapitulating the developmental pattern seen in the human heart ($n \geq 4$ hiPSC-CMs in each group were analyzed). Level of expression and the relative ratios of β-AR subtypes are compared with human fetal heart (FH) and human adult left ventricle (LV) and left atrium (LA) ($n = 2$ in human heart groups). Data show means ± SEM. n.s, not significant; *$P < 0.05$ and **$P < 0.005$ *vs.* each hiPSC group; †$P < 0.05$ and ††$P < 0.0005$ between groups marked (1-way ANOVA with Tukey's test).

measured cAMP production and PKA activation at different hiPSC-CM stages using the subtype nonselective β-AR agonist, ISO. ISO-mediated cAMP production dramatically increased, from 31 ± 1.7 pmol/mg protein at d 30 to 294 ± 21.4 pmol/mg protein at d 60, with a further increase at d 90 (Fig. 2*A*). The increase in ISO-mediated cAMP at d 60 was associated with increased expression of β-ARs (β1-ARs and β2-ARs; 10- and 2-fold increase *vs.* d 30, respectively) and of the major cardiac isotypes of ADCY (ADCY5 and ADCY6; 5- and 4-fold increase *vs.* d 30, respectively) (Supplemental Fig. S2*C*).

Activation of PKA downstream pathways was determined by assessing the PKA-specific phosphorylation of 2 key targets: TnI at Ser23/24 and PLN at Ser16. Protein expression of TnI and PLN increased significantly from d 14 to 30, reaching maximal levels by d 60 (Supplemental Fig. S2). Both d 30 and 60 hiPSC-CMs responded to ISO in a time-dependent manner: phosphorylation of TnI and PLN was evident within 5 min, reached maximum by 15 min, and was sustained through 60 min (Fig. 2*B*). Importantly, as hiPSC-CMs matured from d 30 to 60, compared with total protein, levels of phospho-TnI and phospho-PLN increased 4- and 2-fold, respectively (Fig. 2*C*). These ISO-induced phosphorylation events occurred throughout the hiPSC-CM, as visualized with phosphospecific immunostaining (Fig. 2*D*). TnI protein and phospho-TnI were well

incorporated into the cell's sarcomeric structure, whereas PLN and phospho-PLN were concentrated in the perinuclear area, similar to the pattern in fetal cardiomyocytes (CMs; Fig. 2*D* and Supplemental Fig. S3*A*) (22), evidence that the SR is immature and not yet aligned with sarcomeric structure at this stage.

Correlating with the increase in β-AR signaling, chronotropic response to β-AR stimulation increased with time after differentiation. The rate of spontaneous beating with prolonged culture decreased [32 beats per minute (bpm) at d 30 *vs.* 20 bpm at d 90], but ISO increased beating rate by 123% at d 30 and by 161% at d 90 (Fig. 2*E*).

Coupling of β-ARs to downstream targets mediating cardiac remodeling

β-ARs also activate downstream targets involved in cardiac structural remodeling (hypertrophy and fibrosis) as well as mediators of cardiotoxicity, including ERK, Akt, and CaMKII. We found that ISO treatment of hiPSC-CMs increased phosphorylation of ERK, Akt, and CaMKII; however, coupling to these remodeling mediators developed at different times after hiPSC-CM maturation (Fig. 2*B, C*). ERK was maximally phosphorylated by d 30 with no further increase at d 60 and 90. In rodent cells, β-AR-mediated
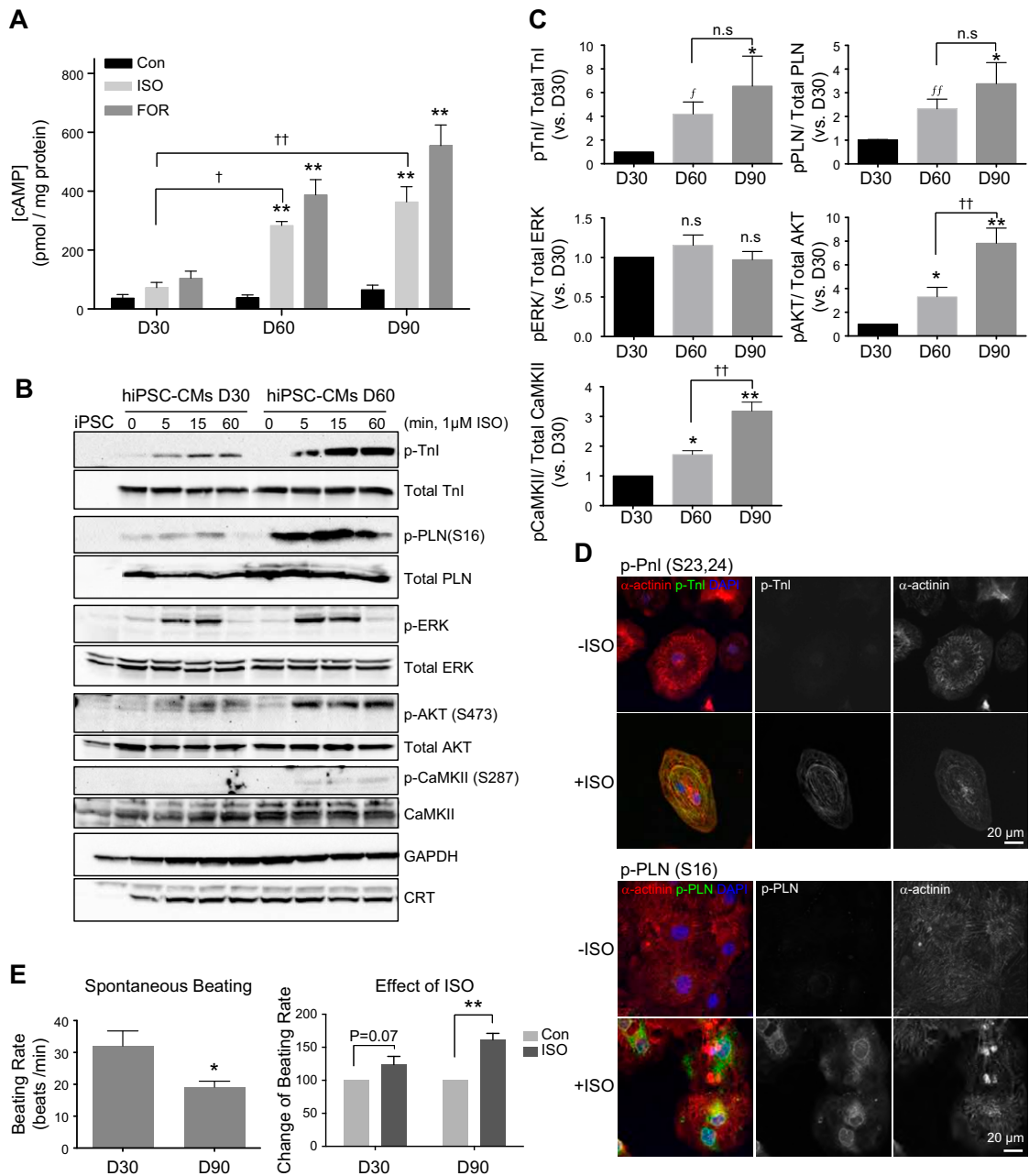
Figure 2. Increased coupling of β-ARs to downstream targets with time after cardiac induction of hiPSC-CMs. *A*) Maturation of cAMP generation. Both ISO-stimulated cAMP generation and maximal ADCY activity induced by forskolin (FOR) increased dramatically from d 30 to 90. Intracellular cAMP was measured with 1 µM ISO or 10 µM FOR after 10 min and normalized to total protein (picomoles per milligram). Data show means ± SEM ($n = 3$ per group). **$P < 0.0005$ *vs.* each control (Con) group; [†]$P < 0.005$ and [††]$P < 0.0005$ *vs.* ISO at d 30 (2-way ANOVA with Sidak's test). *B*) Maturation of β-AR downstream signaling. hiPSC-CMs (d 30 and 60) were stimulated with 1 µM ISO for 0, 5, 15, and 60 min. Key targets of β-AR contractile signaling (PLN and TnI) and of remodeling/cell survival signaling (ERK, Akt, and CaMKII) were immunoblotted for total and phosphoproteins and were compared in d 30 and 60 hiPSC-CMs. GAPDH was used as a loading control. Expression of Ca^{2+} handling proteins (calreticulin [CRT]; SERCA2a, $Cav_{1.2}$, and NCX1) is shown in Supplemental Fig. S2. *C*) Maturation of β-AR–induced phosphorylation of downstream targets. ISO-induced phosphorylation of TnI, PLN, ERK, AKT, and CaMKII was quantified in d 30, 60, and 90 hiPSC-CMs *vs.* total proteins and fold changes compared to d 30. Data show means ± SEM ($n = 3$ per group). n.s, not significant; *$P < 0.05$ and **$P < 0.005$ *vs.* each d 30; [††]$P < 0.05$ (1-way ANOVA with Tukey's test); [f]$P < 0.05$ and [ff]$P < 0.005$ (Student's t test *vs.* d 30). *D*) Cell-wide phosphorylation of contractile proteins was visualized by staining with anti-phospho-TnI or anti-phospho-PLN (both green) before and after ISO (1 µM for 15 min) in d 50 hiPSC-CMs. Sarcomeric α-actinin (red) stains CMs and DAPI (blue) the nucleus. *E*) Effect of ISO on beating rate. Although spontaneous beating rate decreased from d 30 to 90 hiPSC-CMs with *$P < 0.05$ (Student's t test; $n = 10$ each group), the chronotropic response to ISO increased from d 30 to 90 with **$P < 0.0005$ (2-way ANOVA with Sidak's test). Data show means ± SEM.

ERK activation has been linked to transactivation of the epidermal growth factor receptor (23). However, in both early- and late-stage hiPSC-CMs, β-ARs activate Src-dependent ERK phosphorylation but very limited epidermal growth factor receptor-dependent ERK phosphorylation (Supplemental Fig. S4A). In contrast to ERK signaling, phosphorylation of Akt was minimal at d 30 and continued to increase by d 90. Finally, and of critical importance to the use of hiPSC-CMs for cardiotoxicity screening, β-AR activation of CaMKII was almost undetectable at d 30 and only present between d 60 and 90, despite similar levels of CaMKII expression at all stages (Figs. 2B, C, and **6B, D**).

Transition of β-AR subtype signaling during maturation of hiPSC-CMs

We next examined β-AR subtype-specific signaling in hiPSC-CMs to determine how closely it recapitulates the subtype signaling typical of adult CMs. In the adult human heart, β1-ARs are the dominant regulators of functional changes in chronotropy, inotropy, and lusitropy, with β2-ARs having a minimal effect (24). We treated hiPSC-CMs at different stages with ISO in the presence of the β1-selective antagonist CGP, the β2-selective antagonist ICI, or the β1/β2-nonselective antagonist PRO, and examined cAMP generation (**Fig. 3A**) and PKA activity by assessing the phosphorylation of PLN and TnI (Fig. 3B and Supplemental Fig. S4B) for maturation-dependent effects of antagonists. At d 30, the vast majority of β-AR activity (*i.e.*, cAMP generation and PKA-promoted phosphorylation) was mediated by β2-ARs. By d 60, similar to the changes in receptor expression, β1-AR signaling (CGP-dependent inhibition) increases: representing 0% of cAMP generation d 30 and increasing to $56.8 \pm 6.6\%$ by d 60. A similar increase occurs for PKA-dependent PLN phosphorylation: $15.7 \pm 5.2\%$ (d 30), $49.8 \pm 0.5\%$ (d 60), and $71.0 \pm 6.1\%$ (d 90), although by d 90, there were minor increases in functional switching (β2 to β1) for cAMP generation and TnI phosphorylation (Fig. 3). The physiologic significance of this signaling dominance of β2-ARs in early hiPSC-CMs was confirmed by data showing that ICI blocked the ISO-induced positive chronotropic effect in d 30 hiPSC-CMs, but not in d 90 cells (Supplemental Fig. S4B). Of note, adding ICI in the absence of ISO produced inverse agonism, decreasing beating rate below baseline, the first time that this signaling mechanism has been demonstrated in human cardiac cells (25).

Development of functional β-AR compartmentalization in late-stage hiPSC-CMs

The lack of β-AR subtype specificity for activation of PKA downstream mediators (above) represents a dramatic difference between hiPSC-CMs and studies using adult murine CMs. In adult rodent cells, β1-AR–induced PKA signaling is global, whereas β2-ARs do not induce cell-wide activation of PKA, as evidenced by lack of PLN phosphorylation (Fig. 3B, rightmost panels). However, neonatal rodent CMs, which lack compartmentalization, manifest β2-AR–dependent phosphorylation of PLN and

TnI, despite much lower activation compared to adult CMs (26, 27). Whether this major difference in hiPSC-CM β2-AR signaling compartmentalization represents a species or a maturational difference was the subject of our next studies.

A characteristic of mature CMs is a well-aligned sarcomeric structure with an organized T-tubule system. In adult CMs, compartmentalization of β2-AR-cAMP signaling is mediated by structural restriction of the β2-AR to caveolae/T tubules (28) and by localized activity of cAMP-hydrolyzing phosphodiesterases (29). Cav3 induces formation of caveolae, which plays an important role as a cell signaling hub and in the developing T-tubule system (30, 31). We found maturation of caveolae in hiPSC-CMs, as reflected by Cav3 gene and protein expression, which dramatically increased at d 60 and further increased by d 90 (**Fig. 4A, B**). Another component of cardiac caveolar structure, muscle-restricted coiled-coil protein/Cavin4 (32) also increases by d 60–90 (Fig. 4A). Immunostaining of more than d 60 hiPSC-CMs shows the presence of Cav3 clusters at the cell membrane (Fig. 4C), suggesting development of a specialized caveolar membrane subdomain at the later stages of maturation.

To evaluate the functional consequences of caveolar structures for compartmentalization of β2-AR signaling, we utilized the cholesterol-extracting agent, methyl-β-cyclodextrin (MβCD), to disrupt caveolae. In more than d 60 hiPSC-CMs, MβCD scattered the clustered Cav3 structures (Fig. 4D) and increased ISO-induced phospho-PLN and phospho-TnI, compared to ISO without MβCD ($143 \pm 13\%$ and $116 \pm 4\%$, respectively) (Fig. 4E), suggesting that caveolae begin to functionally restrict β-AR signaling in cells at this stage (more than d 60).

Internalization of β2-ARs in response to agonist is functional in early-stage hiPSC-CMs

A key metric of a functional β-AR signaling system is its ability to adjust to prolonged agonist exposure by receptor desensitization and down-regulation. A mechanism for β2-AR down-regulation is *via* β-arrestin/clathrin-mediated endocytic pathways, which also initiate β-arrestin–mediated remodeling signaling (33). To examine subtype and maturational differences in internalization, we transfected Flag-tagged β1-ARs or β2-ARs into d 30 and 90 hiPSC-CMs and incubated the cells with 10 μM ISO for 1 h. At both d 30 and 90, β2-ARs rapidly internalized into endosome-like vesicles, but β1-ARs showed minimal internalization (**Fig. 5A**), recapitulating the subtype specificity seen in other cell types [*e.g.*, human embryonic kidney 293 cells (Fig. 5A, left panel) and neonatal mouse CMs] (34). In d 90 hiPSC-CMs (more mature in sarcomere arrangement, SR and caveolae formation), internalization was less efficient: 52% at d 90 *vs.* 90% at d 30 for β2-ARs, and 3 *vs.* 13.5% for β1-ARs.

Cardiotoxicity induced by chronic stimulation of β-ARs is a late-onset process

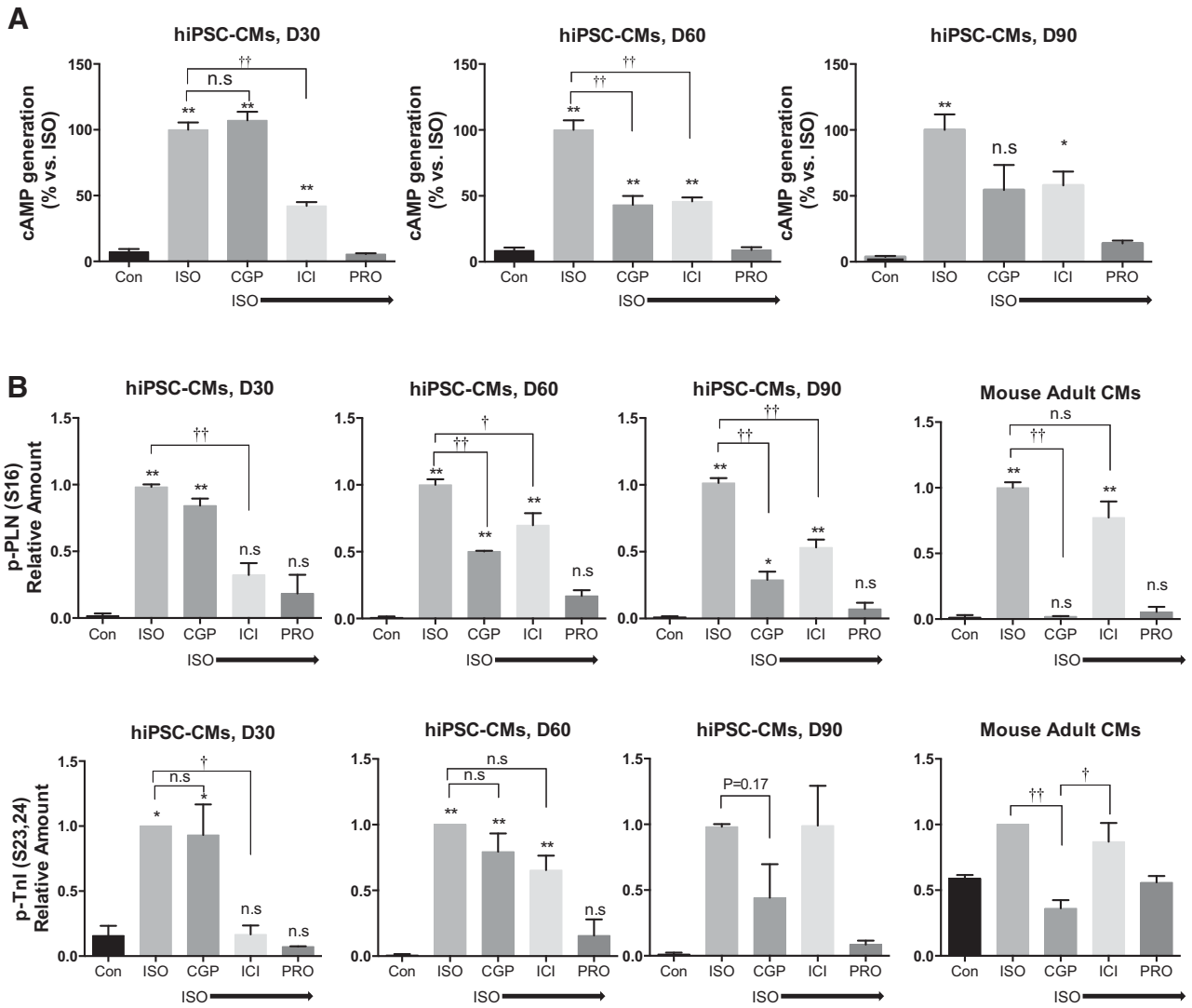β-ARs couple to cardiotoxic signaling pathways with higher doses or longer duration of agonist exposure, providing a

Figure 3. Transition of subtype-specific β-AR signaling from β2 to β1 with prolonged time after cardiac induction. Cells at d 30, 60, and 90 were stimulated with 1 μM ISO alone (ISO) or in the presence of 1 μM of the β-antagonists CGP (β1 selective), ICI (β2 selective), or PRO (nonspecific) for 15 min. *A*) The contribution of β1-AR stimulation to total cAMP generation increased with time after cardiac induction as did the contribution of β1- *vs.* β2-AR stimulation. *B*) PKA activation shows a similar maturation with time after induction. PKA activity was assessed by phosphorylation of the downstream targets (Ser16 pPLN and Ser23/24 pTnI) and compared to results with murine adult CMs (rightmost panel). Data show means ± SEM from 3 independent experiments (mouse adult CMs from duplicate). n.s, not significant; *$P < 0.05$ and **$P < 0.005$ *vs.* each control group; †$P < 0.05$ and ††$P < 0.005$, between groups (1-way ANOVA with Tukey's test).

mechanism by which enhanced sympathetic activity contributes to disease progression in cardiomyopathy (11). We found that this coupling occurs in hiPSC-CMs, but importantly, only during very late stages of maturation (d 90). Cell death (assessed by MTS assay) was induced by β-AR signaling at different stages using escalating doses of ISO (1, 10, and 100 μM) for 48 h. Cardiotoxic signaling showed a dramatic dependence on time after hiPSC-CM induction. At d 30, a time point at which most previously published hiPSC-CM studies have been performed, there was no evidence of ISO-induced cell death at any dose. At d 60, ISO began to induce cell death, but this reached significance only at the highest dose (100 μM). Only at d 90 did hiPSC-CMs show dose-dependent toxicity to ISO, which was reversed by the

nonselective β-blocker, PRO (Fig. 6*A*). DOX cytotoxicity was assessed in different-stage hiPSC-CMs as a positive control for ISO-induced cytotoxicity experiments. Various concentrations of DOX (0.1, 0.5, 1, and 5 μM) were administered as in the ISO cytotoxicity experiment. In contrast to ISO, DOX toxicity was evident as early as d 30; however, hiPSC-CMs did become more sensitive to DOX at later stages (Fig. 6*B*).

Prior studies have proposed CaMKIIδ as a principal mediator of the cardiotoxic effects of β-AR stimulation (35, 36). In hiPSC-CMs, CaMKIIδ protein expression reached a maximal level by d 30 (Fig. 6*C*); however, coupling to β-ARs took much longer to establish. There was minimal CaMKII activation by ISO at d 30 (Figs. 2*B* and 6*D*), consistent with the lack of cardiotoxic effect of
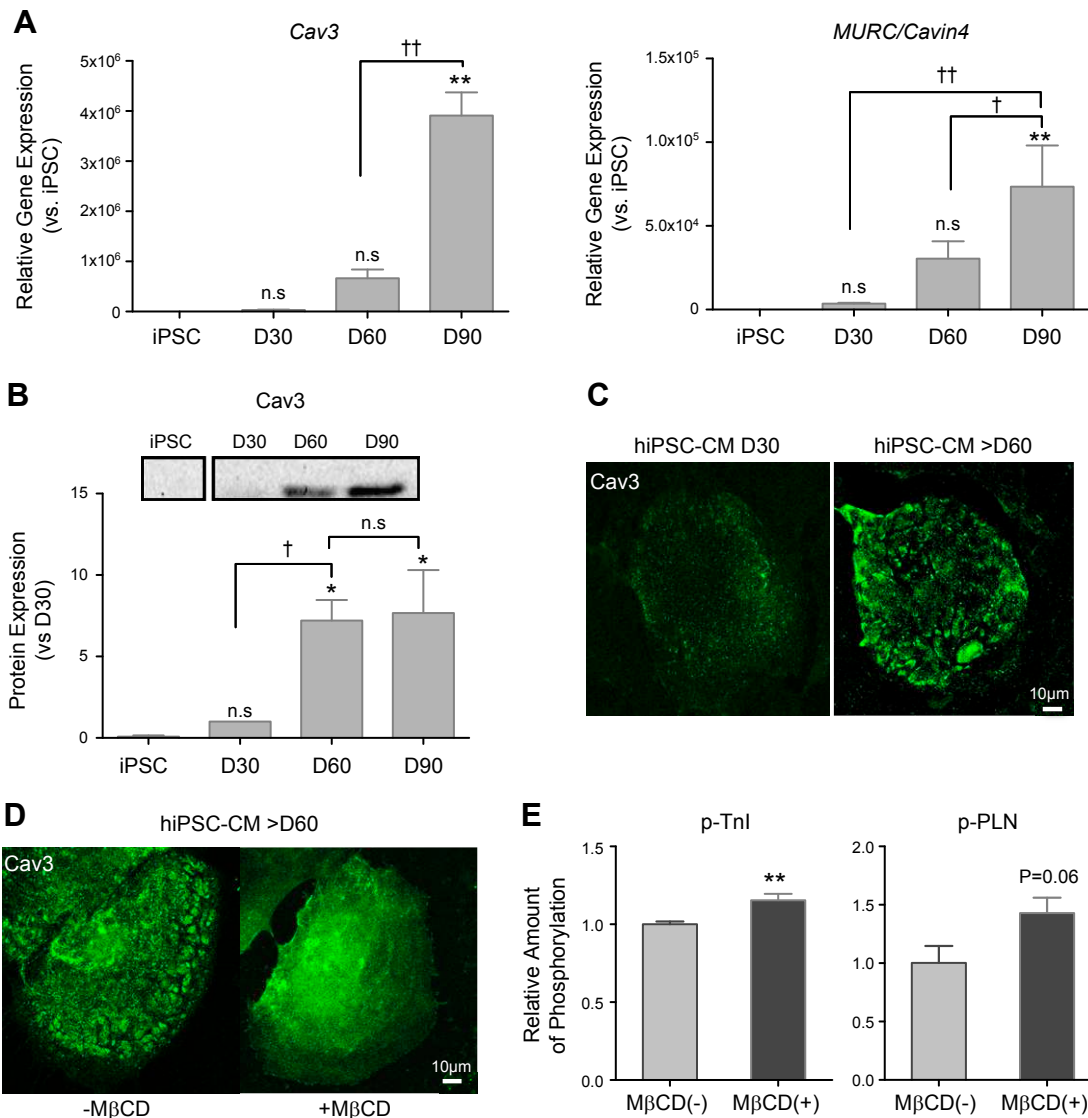
Figure 4. Functional maturation of caveolar structure and β-AR signaling compartmentalization. *A*) Gene expression of Cav3 and muscle-restricted coiled-coil protein (MURC)/Cavin4 increased dramatically with time, with the greatest increase in *Cav3* expression delayed until d 90. Shown are data from iPSCs and in different-stage hiPSC-CMs (d 30, 60, and 90). *B*) Protein expression of Cav3 was assessed and normalized to d 30. Representative immunoblot (from a continuous membrane) shows the largest increase in protein expression at d 60 and 90. Data from $n \geq 3$ per group show means ± SEM. n.s, not significant; *$P < 0.05$ and **$P < 0.005$ *vs.* iPSC; †$P < 0.05$ and ††$P < 0.0005$ between groups by 1-way ANOVA with Tukey's test for (*A*) and (*B*). *C*) Early maturation of caveolar structures (shown by Cav3 cluster immunofluorescent staining) only in more than d 60 hiPSC-CMs. *D*) The cholesterol-extracting agent, MβCD (2 mM for 30 min), disrupts clustered staining of Cav3 in more than d 60 hiPSC-CMs. *E*) Caveolar disruption enhances ISO-stimulated downstream signaling in more than d 60 hiPSC-CMs. After preincubation with MβCD, cells were stimulated with ISO (1 μM for 15 min) then analyzed for phosphorylation of TnI and PLN. Relative amounts of phosphorylation from 4 independent experiments were graphed *vs.* levels without MβCD incubation, respectively. Data are shown as means ± SEM. **$P < 0.005$ (Student's *t* test).

ISO at this time point. Only at later times after cardiac induction (d 60–90) did ISO induce CaMKII activation (Fig. 6*D*), consistent with the time of onset of cardiotoxicity; both CaMKII activation and cell death were blocked by PRO. This effect was mediated by both β1 and β2-ARs because it was not blocked by either β1- or β2-AR–selective antagonists alone, another difference between hiPSC-CMs and data obtained in rodent cells (35, 36). Furthermore, as an emerging mediator of pathologic β-AR signaling to CaMKII, we show that Epac2 expression gradually increases by d 90, whereas, in contrast, Epac1 is stably

expressed. A selective activator of Epac (8CTP-2Me-cAMP) induced cell death only in d 90, not in d 30, hiPSC-CMs (Supplemental Fig. S4*C, D*), suggesting one potential mechanism for the delay in β-AR-CaMK-cell death signaling.

Multiple GPCRs

Many signaling pathways have been identified as regulators of cardiac remodeling, including other GPCRs, stress
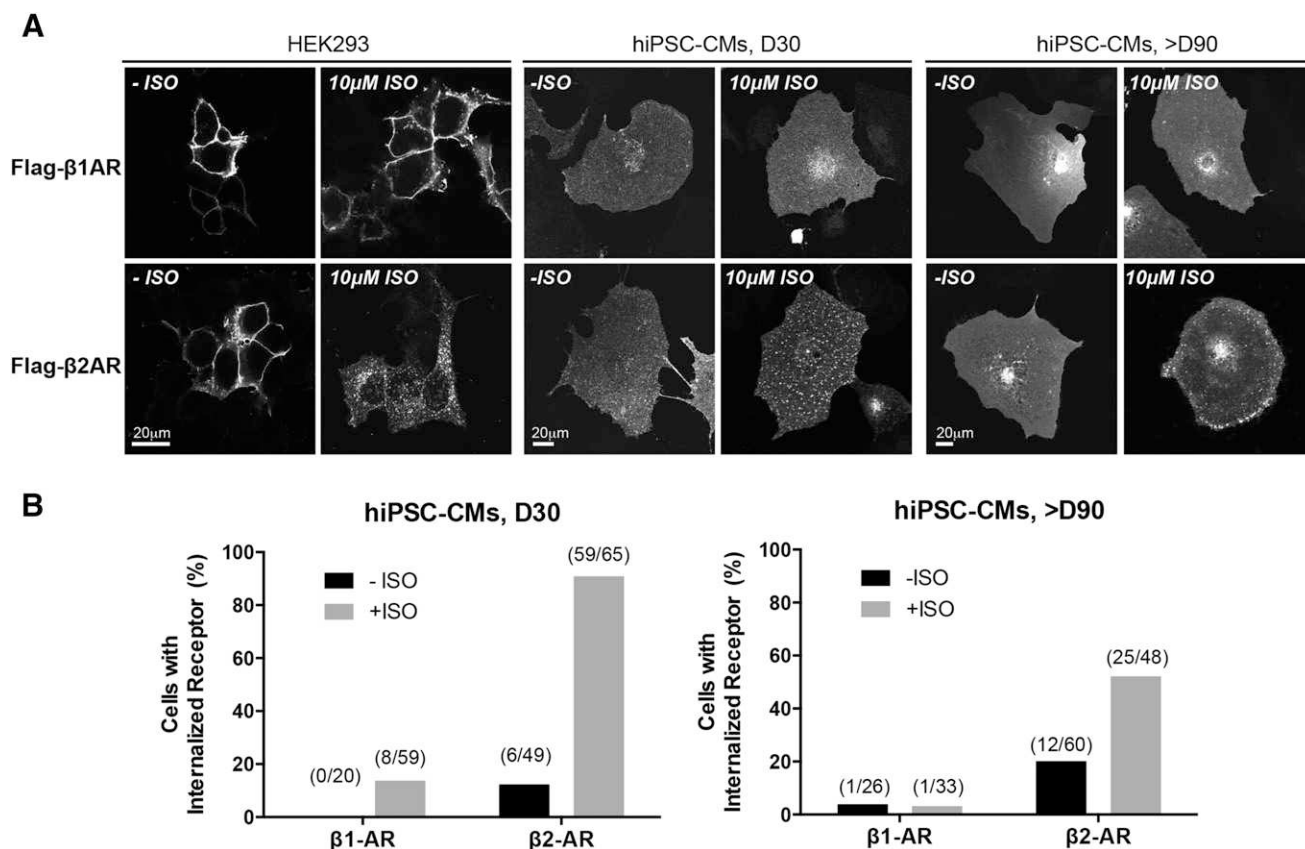
Figure 5. Internalization is a major mechanism for β2-AR, but not β1-AR, down-regulation in both early- and late-stage hiPSC-CMs. *A*) Flag-β1-ARs or Flag-β2-ARs were transfected into human embryonic kidney (HEK)293 cells and hiPSC-CMs (d 30 and 90). In the absence of agonist stimulation, both receptors are expressed on the plasma membrane. With ISO (10 μM for 1 h), only Flag-β2-ARs are efficiently internalized to intracellular endosome-like vesicles. *B*) Quantification of the number of cells harboring internalized receptors from 2 independent experiments.

receptors, receptor tyrosine kinases, the TGF-β/activin family, and TNF. We chose to first focus on the β-AR pathway, because of its central importance in the pathogenesis of heart failure, as well as its role for >3 decades as a prototype to understand the function of G protein-coupled signaling systems. To demonstrate that our findings regarding maturation of β-AR signaling apply to other GPCRs, we performed a global assessment of GPCR expression in hiPSC-CMs using a TaqMan GPCR array platform, representing 342 total GPCRs. We found that many GPCRs follow a similar maturational pattern to that of β-ARs from d 0 through 90 after cardiac induction (Fig. 6*E* and Supplemental Table S1).

Accelerated maturation of β-AR signaling through biomechanical patterning

A hallmark that differentiates mature (adult) from immature (embryonic/fetal) CMs is their rod-shaped morphology, highly aligned sarcomeres, and primarily longitudinal contraction. Although hiPSC-CMs lack this longitudinal structure, several groups have demonstrated that culturing in 2-dimensional (2D) or 3-dimensional arrays can force hiPSC-CMs to adopt a more mature morphology. We hypothesized that maturation of β-AR signaling could be accelerated

along with morphologic changes induced by growing cells in aligned cultures. At 30 d postcardiac induction, hiPSC-CMs were replated on PDMS microgrooves (30/30 μm) and studied at d 55 to evaluate the effect of alignment on β-AR signaling. Nonpatterned PDMS was used as a control. Cells on the control substrate had a random orientation and a circular, cobblestone-like morphology (**Fig. 7***A*). In contrast, cells cultured on microgrooved substrates elongated their cytoskeleton along the direction of the grooved channels. Gene expression of β1- and β2-ARs and Cav3 increased compared to control cells on flat surfaces, most notably β1-ARs (which increased >2-fold) (Fig. 7*B*). TnI and PLN expression as well as ISO-induced phosphorylation of TnI and PLN were also significantly increased on patterned cells (Fig. 7*C, D*). This accelerated maturation of cell signaling was confirmed in an independent set of experiments in which cells were replated on microgrooved PDMS at a later time point (d 40) and studied at d 72 (Supplemental Fig. S5).

DISCUSSION

Despite the great potential for hiPSC-CMs, prior studies have not fully characterized the components, functionality, and physiologic regulation of cell signaling systems
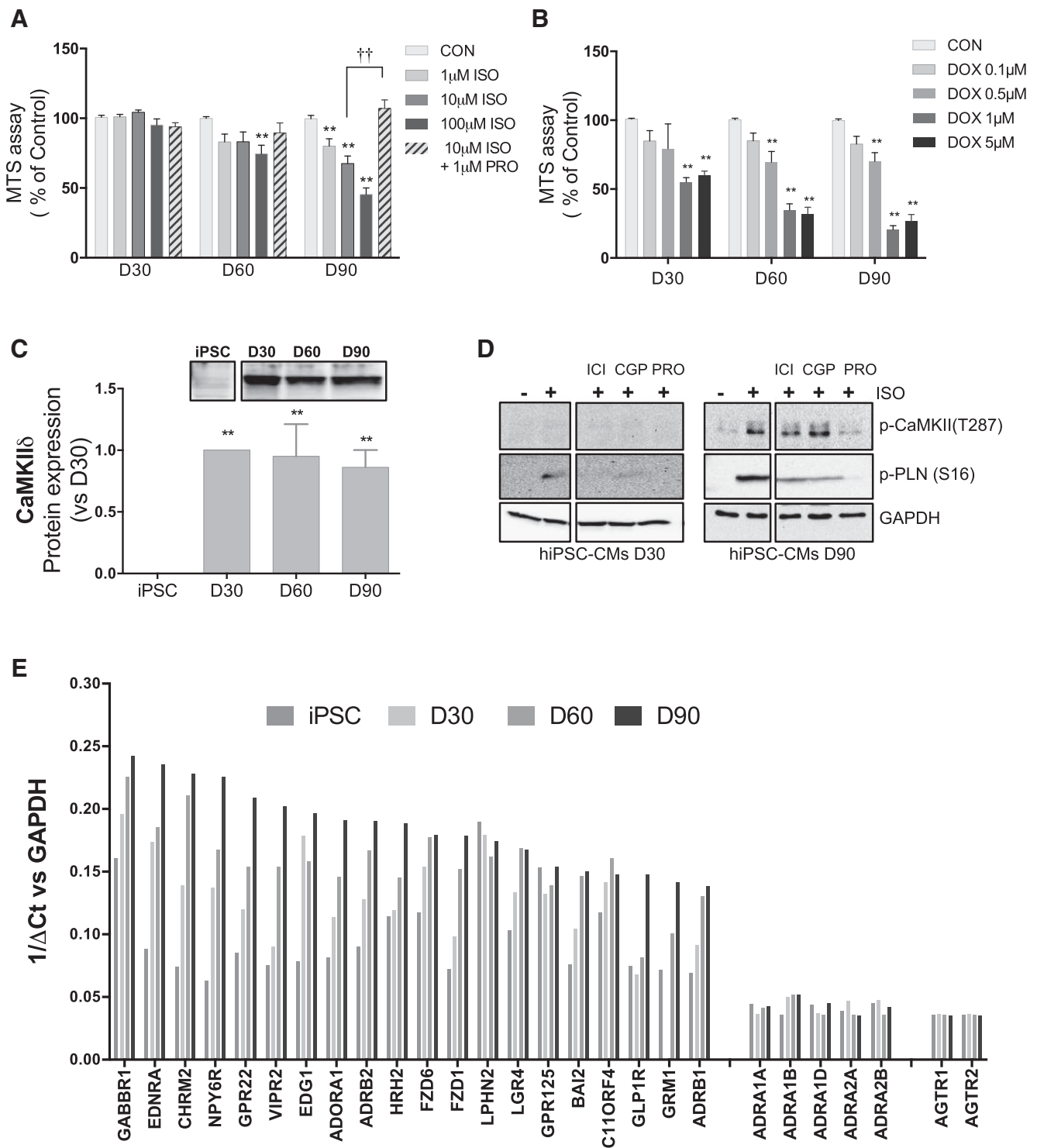
Figure 6. Maturation of β-AR–induced cardiotoxicity occurs only in late-stage hiPSC-CMs. *A*) Different-stage hiPSC-CMs were treated with a cardiotoxic ISO regimen (1, 10, or 100 μM for 48 h), and cell viability was measured with the (MTS) assay. The nonspecific β-antagonist (PRO) was added to confirm the specificity of the cardiotoxic effect for β-ARs. ISO cardiotoxicity was not present at d 30, occurred only at the highest concentration at d 60, and was more fully developed only by d 90. CON, control. *B*) To determine whether this early lack of cardiotoxicity was specific to β-AR stimulation, DOX cytotoxicity was assessed with various concentrations of DOX (0.1, 0.5, 1, and 5 μM) using the same procedure as in the ISO cytotoxicity experiment. In contrast to ISO, DOX toxicity was evident as early as d 30; however, hiPSC-CMs did become more sensitive to DOX at later stages. Data show means ± SEM ($n \geq 3$ independent experiments). **$P < 0.005$ *vs.* Con in each group, ††$P < 0.005$ by 2-way ANOVA with Tukey's test for (*A*) and (*B*). *C*) CaMKIIδ protein (normalized to d 30) was expressed as early as d 30 hiPSC-CMs, with no further increase at later time points. Data are shown as means ± SEM. **$P < 0.0005$ *vs.* iPSC by 1-way ANOVA with Tukey's test. *D*) Despite protein expression at all stages, robust ISO-induced phosphorylation of CaMKII (Thr287) does not occur until d 90,

(continued on next page)

responsible for functional and pathologic changes in CMs, aspects that are especially critical for drug-testing applications. In the current study, we utilized β-AR signaling as a well-known prototype and demonstrated that its functional and remodeling roles are differentially established at distinct time points after cardiac induction. At d 30, β2-AR signaling is dominant, reflecting a relative immaturity of hiPSC-CMs. By d 60, a transition to downstream signaling by the β1-AR represents a more "adult-like" phenotype. Even by d 90, though, β1-AR expression does not fully recapitulate the pattern seen in adult human ventricles. Importantly, there is a striking divergence between functional and remodeling signaling, in that cardiotoxicity induced by sustained β-AR signaling, a key pathophysiologic mechanism in heart failure, only appears well developed by d 90 (Supplemental Fig. S6). This distinction would not have been evident had we examined gene or protein expression alone because CaMKII was expressed at all time points but only functionally coupled to β-ARs at a later stage. Because β-AR signaling shows a distinct time-dependent maturational pattern after cardiac induction, we propose that future studies should use β-AR signaling as a readout for hiPSC-CM functional maturity, along with the more commonly used assays of contractile protein expression, sarcomere morphology, and ion channel function.

β-AR subtype maturation and compartmentalization in hiPSC-CMs: immaturity vs. species divergence

The differential regulation of signaling by β1- vs. β2-AR subtypes during hiPSC-CM maturation is consistent with studies from rodent cells showing that the β2-AR activates cAMP-mediated contraction only in neonatal CMs, whereas β1-AR signaling is more prominent in the adult (37). In contrast, in hiPSC-CMs, even at 90 d, both β-ARs are coupled to cAMP activation and phosphorylation of downstream targets. Although only limited studies have been performed with adult human *myocardium*, intriguingly, such studies have also shown that both β1 and β2-ARs phosphorylate PLN and TnI, although the β1-AR–mediated cAMP increase is more tightly coupled to contractility (38, 39). Those results and the ones here imply that understanding of β-AR subtype signaling based on rodent studies may not reflect their roles in the human heart.

We found other key differences between hiPSC-CMs and adult rodent CMs (*e.g.*, restriction of β2-AR signaling to caveolae T-tubule regions and inability to phosphorylate certain downstream mediators, such as PLN) (28). Lack of compartmentalization of β2-AR signaling has been observed in the absence of a developed T-tubule system in neonates (immaturity) or in the presence of T-tubular disorganization (pathologic processes) (26, 40). Although we demonstrate maturation of β-AR compartmentalization after cardiac differentiation, the degree of this compartmentalization is less than that in rodent cells. The persistent coupling of β2-ARs to downstream effectors in d 90 hiPSC-CMs could be reflective of a still immature signaling system or could reflect a species difference between rodent and human CMs, along with others that include resting heart rate (600 *vs.* 60 bpm), dominant MHC isoform (α- *vs.* β-MHC), and extent of cytosolic Ca^{2+} reuptake by SERCA2a (92 *vs.* 70%). These species differences and the failure of murine models to recapitulate human disease (41, 42) provide further support for the use of hiPSC-CMs to study human cardiac disease mechanisms.

β-AR down-regulation/internalization

One of the key features of mature β-AR signaling is down-regulation/desensitization after prolonged agonist exposure. β1-ARs are more resistant to endocytosis, whereas β2-ARs are readily internalized *via* clathrin-mediated endocytosis (33). Knowledge of β-AR down-regulation mechanisms derives mostly from studies with rodent CMs or non-CM cell lines. Here, we show that β2-ARs are internalized after ISO exposure in both early- and late-stage hiPSC-CMs. The pattern of endocytic vesicles harboring β2-ARs is different in early- *vs.* late-stage hiPSC-CMs, changing from a cell-wide distribution to more membrane specific, possibly reflecting enhanced caveolae formation. These results confirm that hiPSC-CMs can be a useful model to understand the role of the uncoupling of β-AR signaling in the development of diseases such as cardiomyopathy, in which catecholamine-induced down-regulation is a secondary mechanism. The specific mechanisms that mediate internalization of β-ARs in human CMs can be further studied, including whether *via* caveolae *vs.* clathrin-mediated endocytosis or recycling compared to degradative pathways after internalization (33, 43).

Maturation of cardiotoxicity signaling

Persistent activation of β-ARs in patients with heart failure is one of the principal mechanisms inducing secondary neurohormonal pathology, leading to adverse cardiac remodeling and myocyte death. β-Blockers have thus become a mainstay of heart failure management (13). The role of β-AR signaling in cardiotoxicity has not previously been demonstrated in hiPSC-CMs, and most studies have been performed using very early-stage hiPSC-CMs (d 20–30). We show that the deleterious effects of β-AR signaling only become fully active in much later-stage (d 90) hiPSC-CMs, which is consistent with the observation in rodents that mature (adult) CMs are more sensitive to sustained β-AR activation than immature (neonatal) CMs (44). Our findings that β-ARs only activate CaMKII (a critical mediator of the detrimental

paralleling the onset of ISO cardiotoxicity. At d 30 and 90, hiPSC-CMs were stimulated with ISO (1 μM for 15 min) with or without ICI, CGP, or PRO (1 μM). The effect of specific antagonists on the ISO response was compared to phosphorylation of PLN. *E*) Changes in expression over time of the 20 GPCRs with the highest level of mRNA expression at d 90. Data are presented as $1/(\Delta C_t)$ values *vs.* GAPDH expression at 4 time points (d 0, 30, 60, and 90), measured *via* TaqMan GPCR arrays. Corresponding ΔC_t values for each receptor are listed in Supplemental Table S1. Higher values of $1/\Delta C_t$ indicate higher mRNA expression.
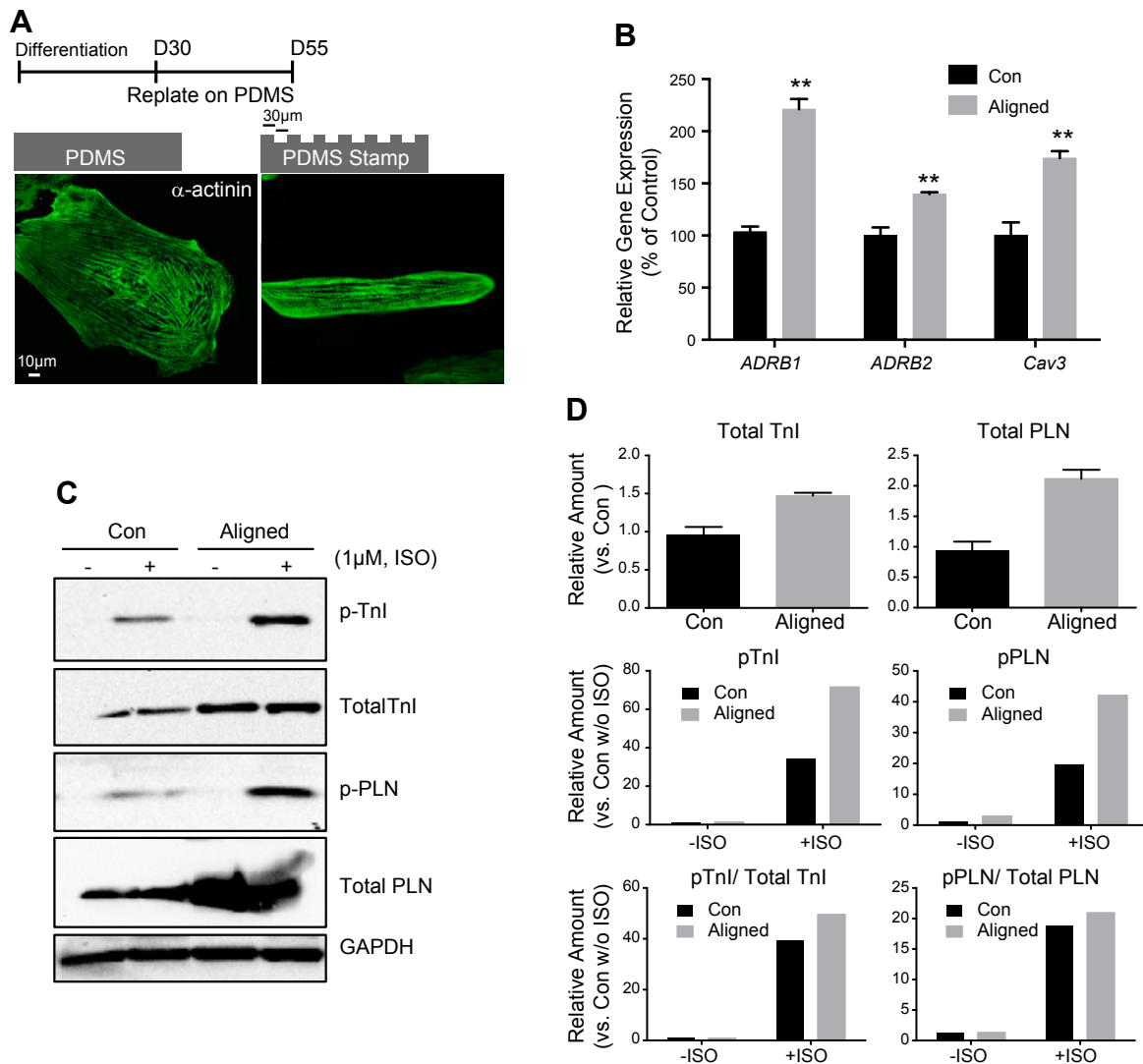
Figure 7. Accelerating maturation of hiPSC-CM β-AR signaling by biomechanical patterning on an aligned microgrooved device. *A*) Schematic protocol for fabrication of PDMS substrate and micrograph show α-actinin staining in nonpatterned *vs.* patterned hiPSC-CMs. *B*) Aligning cells dramatically increases gene expression of β1- and β2-ARs and Cav3 compared to nonpatterned cells. Aligned, patterned cells. Data are shown as means ± SEM. **$P < 0.005$ *vs.* nonpatterned control cells (con) in each gene by 2-way ANOVA with Sidak's test. *C, D*) Maturation of β-AR signaling (phosphorylation of TnI and PLN) is also accelerated by cell alignment. Cells cultured on PDMS were treated with ISO (1 μM for 15 min) and analyzed with immunoblotting against TnI and PLN for both total and phosphoprotein. GAPDH was used as a loading control.

effects of chronic β-AR signaling) at d 90 parallel the development of ISO-induced cardiotoxicity in hiPSC-CMs. Prior studies suggest that sustained β-stimulation activates apoptosis in adult ventricular CMs (11, 45) through CaMKII activation (46, 47), primarily through the β1-AR. However, most of these studies have been done in rodent models, and our data in human cells show no subtype-specific regulation of CaMKII in hiPSC-CMs, even at d 90 (Fig. 6*D*). Similar to our data on compartmentalization of β2-AR signaling, this may reflect a true species divergence or simply that these cells are still immature in their differentiation of β1 *vs.* β2 subtype specificity (35, 36, 48).

Mechanisms by which β-ARs activate CaMKII have been well documented, so we have not replicated all of these pathways, including cAMP/PKA effects on Ca^{2+} channels, increasing [Ca^{2+}]$_i$ and calmodulin activation (49), and

through Epac, a cAMP effector, and β-arrestin (50–52). Epac1 is recruited to the β-arrestin/CaMKII/β1-AR complex on the plasma membrane, activates CaMKII (52), and mediates hypertrophy through the CaMKII-histone deacetylase axis, whereas Epac2 induces SR Ca^{2+} leak and arrhythmia through CaMKII-RyR2 posttranslational modifications (51, 53). Although Epac-mediated CaMKII activation has not been demonstrated in the human heart, in failing human hearts with increased sympathetic activation, CaMKII expression and activity are increased along with RYR2 phosphorylation (Ser2815) at the CaMKII site, accompanied by SR Ca^{2+} leak, which can be blocked by CaMKII inhibition (54, 55). We show that hiPSC-CMs progressively increase expression of total Epac from d 30 through 90, resulting in Epac-induced cell death only in the later-stage cells (Supplemental Fig. S4*C, D*). Further studies to understand the parallels in

late CaMKII activation with β-AR and Epac-mediated cardiotoxicity in late-stage hiPSC-CMs are warranted.

Alterations in SR/Ca^{2+} handling (through PLN) have also been proposed as mediating chronic β-AR–induced cytotoxicity (56), suggesting that immaturity of SR/Ca^{2+} regulation could also be a factor influencing maturation of β-AR cardiotoxicity in hiPSC-CMs. We show that maturation of the contractile machinery (*e.g.*, α-actinin, TnT, and TnI) occurs early in hiPSC-CMs (d 30), whereas expression of the SR/Ca^{2+} cycling machinery, especially components for dyad/triad formation between junctional SR and T tubules (CASQ2 and Cav3), occurs later (d 60–90). Although lacking the adult CM rod-like shape, hiPSC-CMs by d 90 begin to develop better alignment of SR-associated proteins (SERCA2a and PLN) with sarcomeric structure (Supplemental Fig. S3*B*).

The immaturity of β-AR signaling in hiPSC-CMs early after cardiac differentiation (d 30) suggests that studies using cells at this stage to examine mechanisms of cardiomyopathies may miss critical pathologic signaling events that contribute to disease development in the postnatal human heart. Of equal importance, studies of drug cardiotoxicity in earlier-stage cells risk underestimating or perhaps missing this toxicity. Other remodeling mechanisms (*e.g.*, matrix metalloproteinases, cytokines, α-adrenergic receptors, and angiotensin II receptors) also need to be fully assessed before application of drug efficacy/cardiotoxicity screening in hiPSC-CMs can be performed with confidence. Although we focused in the present study on β-AR–induced remodeling, we found the expression of other key GPCRs (*e.g.*, angiotensin II receptors and α-adrenergic receptors) to be quite low in hiPSC-CMs, with the only significant increase over 90 d occurring in α1$_B$-ARs (Fig. 6*E* and Supplemental Table S1), which crosstalk with β-ARs to induce cardiotoxic responses.

Accelerating maturation of hiPSC-CM signaling using biomechanical patterning

Concern over the immaturity of hiPSC-CMs has motivated the development of several methods to enhance their maturation, including coculture with other cardiac cell types, mechanical loading, electrical stimulation, hormonal stimulation, varying substrate stiffness, and small molecules or micro-RNAs (8, 57, 58). hiPSC-CMs on 2D or 3-dimensional–patterned arrays can enhance their morphologic (rod-shaped morphology) and contractile (force generation) maturity (8, 59). We show that a 2D-culture technique (topographic alignment) that induces structural maturation (longitudinal morphology) of hiPSC-CMs can accelerate the maturation of β-AR signaling, addressing concerns raised by our data about the technical feasibility of culturing hiPSC-CMs for such a prolonged period. Use of microgrooved PDMS channels enhanced expression and function of β-ARs and their downstream effectors, as well as expression of Cav3.

We confirmed our findings in 2 additional hiPSC-CM lines, from different individuals (Supplemental Fig. S1). However, we fully acknowledge that other differentiation protocols may yield different results than we obtained.

It is not our intent to claim that β-AR signaling matures exactly along the time line we have defined in all hiPSC-CM lines but instead to identify general principles of signaling maturation. Given the important role of β-ARs in CM function and remodeling, we propose that β-AR expression and signaling can provide critical information regarding hiPSC-CM signaling in general and could be used, in combination with expression of sarcomeric proteins and sarcomeric structure, as one additional index of hiPSC-CM maturation.

In conclusion, our characterization of the ontogeny of β-AR signaling, a critical signaling system, in hiPSC-CMs reveals a differential maturation of downstream pathways mediating cardiac function (which mature early) compared to those that mediate cardiac remodeling and toxicity (which mature late). Our findings may aid future studies and help establish guidelines for the optimal level of CM maturation based on signaling pathway expression and function, depending on the phenotype being studied. Of particular importance for studies of signaling mechanisms in human disease or that test drug efficacy/toxicity, our data imply that hiPSC-CMs should be studied when components of β-AR signaling are sufficiently mature, a process that may be accelerated by culturing cells on a 2D microgrooved substrate. [Fj]

REFERENCES

1. Takahashi, K., Okita, K., Nakagawa, M., and Yamanaka, S. (2007) Induction of pluripotent stem cells from fibroblast cultures. *Nat. Protoc.* **2**, 3081–3089
2. Itzhaki, I., Maizels, L., Huber, I., Zwi-Dantsis, L., Caspi, O., Winterstern, A., Feldman, O., Gepstein, A., Arbel, G., Hammerman, H., Boulos, M., and Gepstein, L. (2011) Modelling the long QT syndrome with induced pluripotent stem cells. *Nature* **471**, 225–229
3. Yazawa, M., Hsueh, B., Jia, X., Pasca, A. M., Bernstein, J. A., Hallmayer, J., and Dolmetsch, R. E. (2011) Using induced pluripotent stem cells to investigate cardiac phenotypes in Timothy syndrome. *Nature* **471**, 230–234
4. Wang, G., McCain, M. L., Yang, L., He, A., Pasqualini, F. S., Agarwal, A., Yuan, H., Jiang, D., Zhang, D., Zangi, L., Geva, J., Roberts, A. E., Ma, Q., Ding, J., Chen, J., Wang, D.-Z., Li, K., Wang, J., Wanders, R. J. A., Kulik, W., Vaz, F. M., Laflamme, M. A., Murry, C. E., Chien, K. R., Kelley, R. I., Church, G. M., Parker, K. K., and Pu, W. T. (2014) Modeling the mitochondrial cardiomyopathy of Barth syndrome with induced pluripotent stem cell and heart-on-chip technologies. *Nat. Med.* **20**, 616–623

5. Lan, F., Lee, A. S., Liang, P., Sanchez-Freire, V., Nguyen, P. K., Wang, L., Han, L., Yen, M., Wang, Y., Sun, N., Abilez, O. J., Hu, S., Ebert, A. D., Navarrete, E. G., Simmons, C. S., Wheeler, M., Pruitt, B., Lewis, R., Yamaguchi, Y., Ashley, E. A., Bers, D. M., Robbins, R. C., Longaker, M. T., and Wu, J. C. (2013) Abnormal calcium handling properties underlie familial hypertrophic cardiomyopathy pathology in patient-specific induced pluripotent stem cells. *Cell Stem Cell* **12**, 101–113

6. Sun, N., Yazawa, M., Liu, J., Han, L., Sanchez-Freire, V., Abilez, O. J., Navarrete, E. G., Hu, S., Wang, L., Lee, A., Pavlovic, A., Lin, S., Chen, R., Hajjar, R. J., Snyder, M. P., Dolmetsch, R. E., Butte, M. J., Ashley, E. A., Longaker, M. T., Robbins, R. C., and Wu, J. C. (2012) Patient-specific induced pluripotent stem cells as a model for familial dilated cardiomyopathy. *Sci. Transl. Med.* **4**, 130ra47

7. Lundy, S. D., Zhu, W. Z., Regnier, M., and Laflamme, M. A. (2013) Structural and functional maturation of cardiomyocytes derived from human pluripotent stem cells. *Stem Cells Dev.* **22**, 1991–2002

8. Yang, X., Pabon, L., and Murry, C. E. (2014) Engineering adolescence: maturation of human pluripotent stem cell-derived cardiomyocytes. *Circ. Res.* **114**, 511–523

9. Rosenbaum, D. M., Rasmussen, S. G. F., and Kobilka, B. K. (2009) The structure and function of G-protein-coupled receptors. *Nature* **459**, 356–363

10. Lohse, M. J., Engelhardt, S., and Eschenhagen, T. (2003) What is the role of beta-adrenergic signaling in heart failure? *Circ. Res.* **93**, 896–906

11. Communal, C., Singh, K., Pimentel, D. R., and Colucci, W. S. (1998) Norepinephrine stimulates apoptosis in adult rat ventricular myocytes by activation of the beta-adrenergic pathway. *Circulation* **98**, 1329–1334

12. Bernstein, D., Fajardo, G., and Zhao, M. (2011) The role of β-adrenergic receptors in heart failure: differential regulation of cardiotoxicity and cardioprotection. *Prog. Pediatr. Cardiol.* **31**, 35–38

13. Bristow, M. R. (2000) beta-adrenergic receptor blockade in chronic heart failure. *Circulation* **101**, 558–569

14. Germanguz, I., Sedan, O., Zeevi-Levin, N., Shtrichman, R., Barak, E., Ziskind, A., Eliyahu, S., Meiry, G., Amit, M., Itskovitz-Eldor, J., and Binah, O. (2011) Molecular characterization and functional properties of cardiomyocytes derived from human inducible pluripotent stem cells. *J. Cell. Mol. Med.* **15**, 38–51

15. Wu, H., Lee, J., Vincent, L. G., Wang, Q., Gu, M., Lan, F., Churko, J. M., Sallam, K. I., Matsa, E., Sharma, A., Gold, J. D., Engler, A. J., Xiang, Y. K., Bers, D. M., and Wu, J. C. (2015) Epigenetic regulation of phosphodiesterases 2A and 3A underlies compromised β-adrenergic signaling in an iPSC model of dilated cardiomyopathy. *Cell Stem Cell* **17**, 89–100

16. Burridge, P. W., Matsa, E., Shukla, P., Lin, Z. C., Churko, J. M., Ebert, A. D., Lan, F., Diecke, S., Huber, B., Mordwinkin, N. M., Plews, J. R., Abilez, O. J., Cui, B., Gold, J. D., and Wu, J. C. (2014) Chemically defined generation of human cardiomyocytes. *Nat. Methods* **11**, 855–860

17. Lian, X., Hsiao, C., Wilson, G., Zhu, K., Hazeltine, L. B., Azarin, S. M., Raval, K. K., Zhang, J., Kamp, T. J., and Palecek, S. P. (2012) Robust cardiomyocyte differentiation from human pluripotent stem cells via temporal modulation of canonical Wnt signaling. *Proc. Natl. Acad. Sci. USA* **109**, E1848–E1857

18. Schefe, J. H., Lehmann, K. E., Buschmann, I. R., Unger, T., and Funke-Kaiser, H. (2006) Quantitative real-time RT-PCR data analysis: current concepts and the novel "gene expression's CT difference" formula. *J. Mol. Med.* **84**, 901–910

19. Qin, D., Xia, Y., and Whitesides, G. M. (2010) Soft lithography for micro- and nanoscale patterning. *Nat. Protoc.* **5**, 491–502

20. Huang, N. F., Lai, E. S., Ribeiro, A. J. S., Pan, S., Pruitt, B. L., Fuller, G. G., and Cooke, J. P. (2013) Spatial patterning of endothelium modulates cell morphology, adhesiveness and transcriptional signature. *Biomaterials* **34**, 2928–2937

21. Kamakura, T., Makiyama, T., Sasaki, K., Yoshida, Y., Wuriyanghai, Y., Chen, J., Hattori, T., Ohno, S., Kita, T., Horie, M., Yamanaka, S., and Kimura, T. (2013) Ultrastructural maturation of human-induced pluripotent stem cell-derived cardiomyocytes in a long-term culture. *Circ. J.* **77**, 1307–1314

22. Butler, J., Lee, A. G., Wilson, D. I., Spalluto, C., Hanley, N. A., and East, J. M. (2007) Phospholamban and sarcolipin are maintained in the endoplasmic reticulum by retrieval from the ER-Golgi intermediate compartment. *Cardiovasc. Res.* **74**, 114–123

23. Grisanti, L. A., Talarico, J. A., Carter, R. L., Yu, J. E., Repas, A. A., Radcliffe, S. W., Tang, H.-A., Makarewich, C. A., Houser, S. R.,

and Tilley, D. G. (2014) β-Adrenergic receptor-mediated transactivation of epidermal growth factor receptor decreases cardiomyocyte apoptosis through differential subcellular activation of ERK1/2 and Akt. *J. Mol. Cell. Cardiol.* **72**, 39–51

24. Brodde, O. E. (1991) Beta 1- and beta 2-adrenoceptors in the human heart: properties, function, and alterations in chronic heart failure. *Pharmacol. Rev.* **43**, 203–242

25. Zhang, S. J., Cheng, H., Zhou, Y. Y., Wang, D. J., Zhu, W., Ziman, B., Spurgoen, H., Lefkowitz, R. J., Lakatta, E. G., Koch, W. J., and Xiao, R. P. (2000) Inhibition of spontaneous beta 2-adrenergic activation rescues beta 1-adrenergic contractile response in cardiomyocytes overexpressing beta 2-adrenoceptor. *J. Biol. Chem.* **275**, 21773–21779

26. Kuznetsov, V., Pak, E., Robinson, R. B., and Steinberg, S. F. (1995) Beta 2-adrenergic receptor actions in neonatal and adult rat ventricular myocytes. *Circ. Res.* **76**, 40–52

27. Xiao, R. P., Hohl, C., Altschuld, R., Jones, L., Livingston, B., Ziman, B., Tantini, B., and Lakatta, E. G. (1994) Beta 2-adrenergic receptor-stimulated increase in cAMP in rat heart cells is not coupled to changes in Ca^{2+} dynamics, contractility, or phospholamban phosphorylation. *J. Biol. Chem.* **269**, 19151–19156

28. Nikolaev, V. O., Bünemann, M., Schmitteckert, E., Lohse, M. J., and Engelhardt, S. (2006) Cyclic AMP imaging in adult cardiac myocytes reveals far-reaching beta1-adrenergic but locally confined beta2-adrenergic receptor-mediated signaling. *Circ. Res.* **99**, 1084–1091

29. Perry, S. J., Baillie, G. S., Kohout, T. A., McPhee, I., Magiera, M. M., Ang, K. L., Miller, W. E., McLean, A. J., Conti, M., Houslay, M. D., and Lefkowitz, R. J. (2002) Targeting of cyclic AMP degradation to beta 2-adrenergic receptors by beta-arrestins. *Science* **298**, 834–836

30. Ogata, T., Ueyama, T., Isodono, K., Tagawa, M., Takehara, N., Kawashima, T., Harada, K., Takahashi, T., Shioi, T., Matsubara, H., and Oh, H. (2008) MURC, a muscle-restricted coiled-coil protein that modulates the Rho/ROCK pathway, induces cardiac dysfunction and conduction disturbance. *Mol. Cell. Biol.* **28**, 3424–3436

31. Patel, H. H., Murray, F., and Insel, P. A. (2008) G-protein-coupled receptor-signaling components in membrane raft and caveolae microdomains. *Handbook Exp. Pharmacol.* **186**, 167–184

32. Bastiani, M., Liu, L., Hill, M. M., Jedrychowski, M. P., Nixon, S. J., Lo, H. P., Abankwa, D., Luetterforst, R., Fernandez-Rojo, M., Breen, M. R., Gygi, S. P., Vinten, J., Walser, P. J., North, K. N., Hancock, J. F., Pilch, P. F., and Parton, R. G. (2009) MURC/Cavin-4 and cavin family members form tissue-specific caveolar complexes. *J. Cell Biol.* **185**, 1259–1273

33. Lefkowitz, R. J. (1998) G protein-coupled receptors. III. New roles for receptor kinases and beta-arrestins in receptor signaling and desensitization. *J. Biol. Chem.* **273**, 18677–18680

34. Xiang, Y., Devic, E., and Kobilka, B. (2002) The PDZ binding motif of the beta 1 adrenergic receptor modulates receptor trafficking and signaling in cardiac myocytes. *J. Biol. Chem.* **277**, 33783–33790

35. Wang, W., Zhu, W., Wang, S., Yang, D., Crow, M. T., Xiao, R.-P., and Cheng, H. (2004) Sustained beta1-adrenergic stimulation modulates cardiac contractility by Ca^{2+}/calmodulin kinase signaling pathway. *Circ. Res.* **95**, 798–806

36. Zhu, W. Z., Wang, S. Q., Chakir, K., Yang, D., Zhang, T., Brown, J. H., Devic, E., Kobilka, B. K., Cheng, H., and Xiao, R. P. (2003) Linkage of beta1-adrenergic stimulation to apoptotic heart cell death through protein kinase A-independent activation of Ca^{2+}/calmodulin kinase II. *J. Clin. Invest.* **111**, 617–625

37. Slotkin, T. A., Lau, C., and Seidler, F. J. (1994) Beta-adrenergic receptor overexpression in the fetal rat: distribution, receptor subtypes, and coupling to adenylate cyclase activity via G-proteins. *Toxicol. Appl. Pharmacol.* **129**, 223–234

38. Del Monte, F., Kaumann, A. J., Poole-Wilson, P. A., Wynne, D. G., Pepper, J., and Harding, S. E. (1993) Coexistence of functioning beta 1- and beta 2-adrenoceptors in single myocytes from human ventricle. *Circulation* **88**, 854–863

39. Kaumann, A., Bartel, S., Molenaar, P., Sanders, L., Burrell, K., Vetter, D., Hempel, P., Karczewski, P., and Krause, E. G. (1999) Activation of beta2-adrenergic receptors hastens relaxation and mediates phosphorylation of phospholamban, troponin I, and C-protein in ventricular myocardium from patients with terminal heart failure. *Circulation* **99**, 65–72

40. Nikolaev, V. O., Moshkov, A., Lyon, A. R., Miragoli, M., Novak, P., Paur, H., Lohse, M. J., Korchev, Y. E., Harding, S. E., and Gorelik, J. (2010) Beta2-adrenergic receptor redistribution in heart failure changes cAMP compartmentation. *Science* **327**, 1653–1657

41. Bers, D. M. (2002) Cardiac excitation-contraction coupling. *Nature* **415**, 198–205

42. Haghighi, K., Kolokathis, F., Pater, L., Lynch, R. A., Asahi, M., Gramolini, A. O., Fan, G. C., Tsiapras, D., Hahn, H. S., Adamopoulos, S., Liggett, S. B., Dorn II, G. W., MacLennan, D. H., Kremastinos, D. T., and Kranias, E. G. (2003) Human phospholamban null results in lethal dilated cardiomyopathy revealing a critical difference between mouse and human. *J. Clin. Invest.* **111**, 869–876

43. Rapacciuolo, A., Suvarna, S., Barki-Harrington, L., Luttrell, L. M., Cong, M., Lefkowitz, R. J., and Rockman, H. A. (2003) Protein kinase A and G protein-coupled receptor kinase phosphorylation mediates beta-1 adrenergic receptor endocytosis through different pathways. *J. Biol. Chem.* **278**, 35403–35411

44. Slotkin, T. A., Lappi, S. E., and Seidler, F. J. (1995) Beta-adrenergic control of c-fos expression in fetal and neonatal rat tissues: relationship to cell differentiation and teratogenesis. *Toxicol. Appl. Pharmacol.* **133**, 188–195

45. Mann, D. L., Kent, R. L., Parsons, B., and Cooper IV, G. (1992) Adrenergic effects on the biology of the adult mammalian cardiocyte. *Circulation* **85**, 790–804

46. Zhang, R., Khoo, M. S. C., Wu, Y., Yang, Y., Grueter, C. E., Ni, G., Price, Jr., E. E., Thiel, W., Guatimosim, S., Song, L. S., Madu, E. C., Shah, A. N., Vishnivetskaya, T. A., Atkinson, J. B., Gurevich, V. V., Salama, G., Lederer, W. J., Colbran, R. J., and Anderson, M. E. (2005) Calmodulin kinase II inhibition protects against structural heart disease. *Nat. Med.* **11**, 409–417

47. Grimm, M., and Brown, J. H. (2010) β-adrenergic receptor signaling in the heart: role of CaMKII. *J. Mol. Cell. Cardiol.* **48**, 322–330

48. Yoo, B., Lemaire, A., Mangmool, S., Wolf, M. J., Curcio, A., Mao, L., and Rockman, H. A. (2009) Beta1-adrenergic receptors stimulate cardiac contractility and CaMKII activation in vivo and enhance cardiac dysfunction following myocardial infarction. *Am. J. Physiol. Heart Circ. Physiol.* **297**, H1377–H1386

49. Xu, L., Lai, D., Cheng, J., Lim, H. J., Keskanokwong, T., Backs, J., Olson, E. N., and Wang, Y. (2010) Alterations of L-type calcium current and cardiac function in CaMKIIdelta knockout mice. *Circ. Res.* **107**, 398–407

50. Pereira, L., Métrich, M., Fernández-Velasco, M., Lucas, A., Leroy, J., Perrier, R., Morel, E., Fischmeister, R., Richard, S., Bénitah, J. P., Lezoualc'h, F., and Gómez, A. M. (2007) The cAMP binding protein Epac modulates Ca^{2+} sparks by a Ca^{2+}/calmodulin kinase signalling pathway in rat cardiac myocytes. *J. Physiol.* **583**, 685–694

51. Pereira, L., Cheng, H., Lao, D. H., Na, L., van Oort, R. J., Brown, J. H., Wehrens, X. H. T., Chen, J., and Bers, D. M. (2013) Epac2 mediates cardiac β1-adrenergic-dependent sarcoplasmic reticulum Ca^{2+} leak and arrhythmia. *Circulation* **127**, 913–922

52. Mangmool, S., Shukla, A. K., and Rockman, H. A. (2010) beta-Arrestin-dependent activation of Ca(2+)/calmodulin kinase II after beta(1)-adrenergic receptor stimulation. *J. Cell Biol.* **189**, 573–587

53. Métrich, M., Lucas, A., Gastineau, M., Samuel, J. L., Heymes, C., Morel, E., and Lezoualc'h, F. (2008) Epac mediates beta-adrenergic receptor-induced cardiomyocyte hypertrophy. *Circ. Res.* **102**, 959–965

54. Neef, S., Dybkova, N., Sossalla, S., Ort, K. R., Fluschnik, N., Neumann, K., Seipelt, R., Schöndube, F. A., Hasenfuss, G., and Maier, L. S. (2010) CaMKII-dependent diastolic SR Ca^{2+} leak and elevated diastolic Ca^{2+} levels in right atrial myocardium of patients with atrial fibrillation. *Circ. Res.* **106**, 1134–1144

55. Sossalla, S., Fluschnik, N., Schotola, H., Ort, K. R., Neef, S., Schulte, T., Wittköpper, K., Renner, A., Schmitto, J. D., Gummert, J., El-Armouche, A., Hasenfuss, G., and Maier, L. S. (2010) Inhibition of elevated Ca^{2+}/calmodulin-dependent protein kinase II improves contractility in human failing myocardium. *Circ. Res.* **107**, 1150–1161

56. Engelhardt, S., Hein, L., Dyachenkow, V., Kranias, E. G., Isenberg, G., and Lohse, M. J. (2004) Altered calcium handling is critically involved in the cardiotoxic effects of chronic beta-adrenergic stimulation. *Circulation* **109**, 1154–1160

57. Hirt, M. N., Boeddinghaus, J., Mitchell, A., Schaaf, S., Börnchen, C., Müller, C., Schulz, H., Hubner, N., Stenzig, J., Stoehr, A., Neuber, C., Eder, A., Luther, P. K., Hansen, A., and Eschenhagen, T. (2014) Functional improvement and maturation of rat and human engineered heart tissue by chronic electrical stimulation. *J. Mol. Cell. Cardiol.* **74**, 151–161

58. Godier-Furnémont, A. F., Tiburcy, M., Wagner, E., Dewenter, M., Lämmle, S., El-Armouche, A., Lehnart, S. E., Vunjak-Novakovic, G., and Zimmermann, W. H. (2015) Physiologic force-frequency response in engineered heart muscle by electromechanical stimulation. *Biomaterials* **60**, 82–91

59. Rao, C., Prodromakis, T., Kolker, L., Chaudhry, U. A., Trantidou, T., Sridhar, A., Weekes, C., Camelliti, P., Harding, S. E., Darzi, A., Yacoub, M. H., Athanasiou, T., and Terracciano, C. M. (2013) The effect of microgrooved culture substrates on calcium cycling of cardiac myocytes derived from human induced pluripotent stem cells. *Biomaterials* **34**, 2399–2411